

pubs.acs.org/JPCC Article

Cavity-Modified Fermi's Golden Rule Rate Constants from Cavity-Free Inputs

Maximilian A. C. Saller, Yifan Lai, and Eitan Geva*



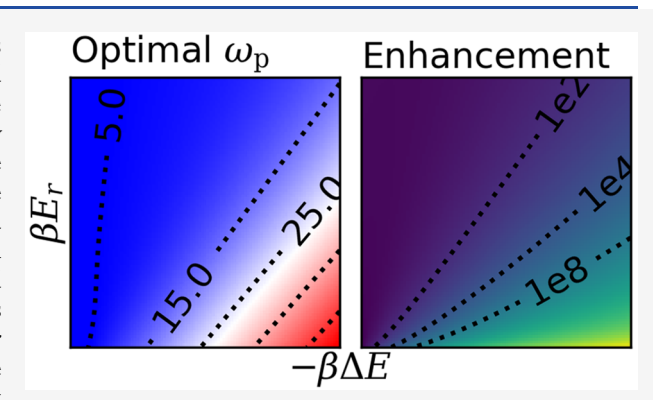
Cite This: J. Phys. Chem. C 2023, 127, 3154-3164



ACCESS |

Metrics & More

ABSTRACT: Equilibrium Fermi's golden rule (FGR) rate constants are commonly used for modeling the kinetics of electronic energy and charge transfer processes in a wide range of molecular systems. The interaction between the electronic degrees of freedom and cavity modes can modify the coupling between electronic states when the molecular system is placed inside a cavity, and thereby alter the corresponding FGR rate constants. In this paper, we present a general-purpose framework for estimating the cavity-induced effect on equilibrium FGR rate constants. We show that cavity-modified equilibrium FGR rate constants can be estimated from inputs obtainable exclusively from a simulation of the cavity-free molecular system, thereby bypassing the need for an explicit simulation of the molecular system inside the cavity. The usefulness of this framework



Article Recommendations

is demonstrated in the Marcus theory limit of equilibrium FGR, and general rules are derived for determining the optimal conditions for cavity-induced Marcus theory rate enhancement.

1. INTRODUCTION

Utilizing light-matter interactions to control chemical processes has been a long-standing theme in physical chemistry. 1-11 Recent experimental work has demonstrated such control for a wide range of chemical phenomena, including chemical reactivity and selectivity, photochemistry, catalysis, and electronic energy and charge transfer, by coupling the molecular electronic and vibrational degrees of freedom (DOF) to the electromagnetic field modes of a cavity that the molecular system is placed into. 12-52 Those experimental advances call for the development of theoretical models for estimating the effect that placing molecular matter inside a cavity has on its behavior and properties. Such models often need to go beyond models previously developed by the quantum optics community, 53-58 which neglect prominent aspects of molecular matter such as transitions between multiple electronic potential energy surfaces, solvent effects, and disorder.

Most recent theoretical studies of molecular matter in cavities assume that strong coupling between the molecular system and cavity modes is necessary for a significant cavity-induced effect to occur. The resulting strong-coupling models necessitate incorporating the cavity DOF into the model and explicitly simulating the molecular system inside the cavity. $^{40,41,45,48-51,59-67}$

However, even relatively weak coupling between molecular and cavity DOF can give rise to significant cavity-enabled effects. This is particularly true in the case of electronic energy and charge transfer processes whose kinetics can be described in terms of equilibrium Fermi's golden rule (FGR) rate constants, which are based on treating the coupling between electronic states as a small perturbation (within the framework of second-order perturbation theory). Coupling between the electronic DOF and cavity modes can modify the coupling between electronic states when the molecular system is placed inside a cavity. Treating this additional electronic coupling as a small perturbation can therefore still give rise to significant modifications of the corresponding FGR rate constants.

In this paper we show that such cavity-modified FGR rate constants can be estimated from inputs obtainable exclusively from a simulation of the cavity-free molecular system, thereby bypassing the need for an explicit simulation of the molecular system inside the cavity. We also demonstrate the usefulness of this framework in the case where the cavity-free kinetics is governed by Marcus theory and derive general, easy-to-use rules for determining the optimal conditions for cavity-induced Marcus theory rate enhancement. We expect this strategy to be particularly useful for the interpretation of experiments that

Received: December 23, 2022 Revised: January 16, 2023 Published: February 1, 2023





target cavity-modified electronic energy and charge transfer rates, since it allows for the effect on the rate resulting from placing the molecular system inside a cavity to be estimated with little to no additional computational cost (compared to the cavity-free case).

The remainder of this paper is organized as follows. The general-purpose framework for estimating the effect of placing the molecular system inside an electromagnetic cavity on equilibrium FGR rate constants is outlined in section 2. A detailed analysis of the case where the equilibrium FGR rate constants are described in terms of Marcus theory, including the derivation of general rules for determining the optimal conditions for cavity-induced rate enhancement, is provided in section 3. Summary of the main results and outlook are provided in section 4.

2. THEORY

Consider a two-electronic-state molecular system which is placed inside a cavity and can undergo an electronic transition between a donor state and an acceptor state. The overall Hamiltonian of such a system has the following form:

$$\hat{H} = \hat{H}_D^{np} |D\rangle\langle D| + \hat{H}_A^{np} |A\rangle\langle A| + \hat{V}_{DA}^{np} [|D\rangle\langle A| + |A\rangle\langle D|]$$
(1)

Here, $|D\rangle$ and $|A\rangle$ are the diabatic donor and acceptor electronic states, respectively; \hat{H}_D^{np} and \hat{H}_A^{np} are the Hamiltonians of the nuclear and photonic DOF when the system is in the donor or acceptor electronic states, respectively, and \hat{V}_{DA}^{np} is the coupling term between the donor and acceptor electronic states, which generally speaking is also an operator in the nuclear+photonic Hilbert space.

Assuming that the photonic and nuclear DOF are coupled to the electronic DOF, but not to each other, which corresponds to a situation where the cavity modes are in resonance with electronic transitions but off-resonance with vibrational transitions, \hat{H}_D^{np} , \hat{H}_A^{np} , and \hat{V}_{DA}^{np} can each be written as a sum of a purely nuclear term and a purely photonic term:

$$\hat{H}_D^{np} = \hat{H}_D^n + \hat{H}^p \tag{2a}$$

$$\hat{H}_A^{np} = \hat{H}_A^n + \hat{H}^p \tag{2b}$$

$$\hat{V}_{DA}^{np} = \hat{V}_{DA}^n + \hat{V}_{DA}^p \tag{2c}$$

Here, the n and p superscripts are used to identify contributions from the nuclear and photonic DOF, respectively. Importantly, such separability is generally valid and arises due to the form of the light-matter Hamiltonian. It should also be noted that the photonic Hamiltonian, \hat{H}^p , is assumed to be independent of the electronic state (i.e., $\hat{H}^p_D = \hat{H}^p_A = \hat{H}^p$). Finally, we note that the cavity-free case corresponds to setting the photonic terms to zero (i.e., $\{\hat{H}^p, \hat{V}^p_{DA}\} \rightarrow 0$) such that

$$\begin{split} \hat{H} &\rightarrow \hat{H}^{m} \\ &= \hat{H}_{D}^{n} |D\rangle \langle D| + \hat{H}_{A}^{n} |A\rangle \langle A| + \hat{V}_{DA}^{n} [|D\rangle \langle A| + |A\rangle \langle D|] \end{split} \tag{3}$$

The superscript m is used to indicate that this is the purely molecular (i.e., cavity-free) Hamiltonian.

The derivation of the equilibrium FGR rate constant is based on treating the electronic coupling term, $\hat{V}_{DA}^{np}[|D\rangle\langle A| + |A\rangle\langle D|]$, as a small perturbation [see eq 1],

within the framework of second-order perturbation theory. It should be noted that the following analysis assumes that both coupling terms in eq 2c can be treated within the framework of second-order perturbation theory, and would therefore not be valid in cases where higher than second-order terms that arise from one coupling term are comparable to the second-order term that arises from the other coupling term. The resulting equilibrium FGR rate constant for the electronic transition from the donor electronic state to the acceptor electronic state is given by $^{68-70}$

$$k_{\mathrm{D}\to\mathrm{A}} = \frac{1}{\hbar^2} \int_{-\infty}^{\infty} \mathrm{d}t \ C_{\mathrm{D}\to\mathrm{A}}(t) \tag{4}$$

where, for the system governed by the Hamiltonian in eq 1, the cavity-modified donor-to-acceptor FGR time correlation function is given by

$$C_{D\to A}(t) = Tr_{n}Tr_{p}[\hat{\rho}_{D}^{eq} e^{i\hat{H}_{D}^{np}t/\hbar} \hat{V}_{DA}^{np} e^{-i\hat{H}_{A}^{np}t/\hbar} \hat{V}_{DA}^{np}]$$
(5)

Here, $Tr_n[...]$ and $Tr_p[...]$ correspond to traces over the nuclear and photonic Hilbert spaces, respectively. We also define for later use the trace over the electronic Hilbert space, $Tr_e[...]$, and the overall trace, $Tr[...] = Tr_eTr_nTr_p[...]$. $\hat{\rho}_D^{eq}$ in eq 5 corresponds to the density operator that describes the state of the nuclear and photonic DOF when the system is at thermal equilibrium in the donor electronic state:

$$\hat{\rho}_{\mathrm{D}}^{\mathrm{eq}} = \frac{\mathrm{e}^{-\beta \hat{H}_{\mathrm{D}}^{np}}}{\mathrm{Tr}_{\mathrm{n}} \mathrm{Tr}_{\mathrm{p}} [\mathrm{e}^{-\beta \hat{H}_{\mathrm{D}}^{np}}]} = \frac{\mathrm{e}^{-\beta \hat{H}_{\mathrm{D}}^{n}}}{Z_{\mathrm{D}}^{n}} \otimes \frac{\mathrm{e}^{-\beta \hat{H}^{p}}}{Z^{p}} = \hat{\rho}_{\mathrm{D,n}}^{\mathrm{eq}} \otimes \hat{\rho}_{p}^{\mathrm{eq}}$$

$$\tag{6}$$

where
$$\beta = 1/k_B T$$
, $Z_D^n = \text{Tr}_n [e^{-\beta \hat{H}_D^n}]$, and $Z^p = \text{Tr}_p [e^{-\beta \hat{H}^p}]$.

It should be noted that the second equality in eq 6 relies on the fact that \hat{H}_D^{np} is separable into a sum of a purely nuclear term and a purely photonic term, $\hat{H}_D^{np} = \hat{H}_D^n + \hat{H}^p$ [see eq 2a]. It should also be noted that the donor-to-acceptor equilibrium rate constant for the cavity-free molecular system is given by

$$k_{\mathrm{D}\to\mathrm{A}}^{m} = \frac{1}{\hbar^{2}} \int_{-\infty}^{\infty} \mathrm{d}t \ C_{\mathrm{D}\to\mathrm{A}}^{m}(t) \tag{7}$$

where for the cavity-free system governed by the Hamiltonian in eq 3, the cavity-free donor-to-acceptor FGR time correlation function is given by

$$C_{\rm D\to A}^{m}(t) = {\rm Tr}_{\rm n}[\hat{\rho}_{{\rm D},n}^{\rm eq} \, {\rm e}^{{\rm i}\hat{H}_{\rm D}^{n}t/\hbar} \, \hat{V}_{\rm DA}^{n} \, {\rm e}^{-{\rm i}\hat{H}_{\rm A}^{n}t/\hbar} \, \hat{V}_{\rm DA}^{n}] \eqno(8)$$

Taking advantage of the separability of \hat{H}_D^{np} , \hat{H}_A^{np} , and \hat{V}_{DA}^{np} into purely nuclear and purely photonic terms [see eqs 2a–2c], it is then straightforward to show that the donor-to-acceptor FGR correlation function can be given in terms of a sum of four terms, each of which consisting of a product of purely nuclear and purely photonic correlation functions:

$$\begin{split} & Tr_{\mathbf{p}}[\hat{\rho}_{\mathbf{p}}^{eq} e^{i\hat{H}^{\mathbf{p}}_{t}/\hbar} e^{-i\hat{H}^{\mathbf{p}}_{t}/\hbar}] Tr_{\mathbf{n}}[\hat{\rho}_{\mathbf{D},\mathbf{n}}^{eq} e^{i\hat{H}_{\mathbf{D}}^{n}t/\hbar} \hat{V}_{\mathbf{D}A}^{n} e^{-i\hat{H}_{\mathbf{A}}^{n}t/\hbar} \hat{V}_{\mathbf{D}A}^{n}] \\ & + Tr_{\mathbf{p}}[\hat{\rho}_{\mathbf{p}}^{eq} e^{i\hat{H}^{\mathbf{p}}_{t}/\hbar} e^{-i\hat{H}^{\mathbf{p}}_{t}/\hbar} \hat{V}_{\mathbf{D}A}^{\mathbf{p}}] Tr_{\mathbf{n}}[\hat{\rho}_{\mathbf{D},\mathbf{n}}^{eq} e^{i\hat{H}_{\mathbf{D}}^{n}t/\hbar} \hat{V}_{\mathbf{D}A}^{n} e^{-i\hat{H}_{\mathbf{A}}^{n}t/\hbar}] \\ & + Tr_{\mathbf{p}}[\hat{\rho}_{\mathbf{p}}^{eq} e^{i\hat{H}^{\mathbf{p}}_{t}/\hbar} \hat{V}_{\mathbf{D}A}^{\mathbf{p}} e^{-i\hat{H}^{\mathbf{p}}_{t}/\hbar}] Tr_{\mathbf{n}}[\hat{\rho}_{\mathbf{D},\mathbf{n}}^{eq} e^{i\hat{H}_{\mathbf{D}}^{n}t/\hbar} e^{-i\hat{H}_{\mathbf{A}}^{n}t/\hbar} \hat{V}_{\mathbf{D}A}^{n}] \\ & + Tr_{\mathbf{p}}[\hat{\rho}_{\mathbf{p}}^{eq} e^{i\hat{H}^{\mathbf{p}}_{t}/\hbar} \hat{V}_{\mathbf{D}A}^{\mathbf{p}} e^{-i\hat{H}^{\mathbf{p}}_{t}/\hbar} \hat{V}_{\mathbf{D}A}^{\mathbf{p}}] Tr_{\mathbf{n}}[\hat{\rho}_{\mathbf{D},\mathbf{n}}^{eq} e^{i\hat{H}_{\mathbf{D}}^{n}t/\hbar} e^{-i\hat{H}_{\mathbf{A}}^{n}t/\hbar}] \end{aligned} \tag{9}$$

Thus, according to eq 9, cavity-modified equilibrium FGR rate constants can be obtained from purely nuclear and purely photonic time correlation functions as inputs and therefore do not necessitate an explicit simulation of the molecular system inside the cavity. Furthermore, as we will show below, the purely photonic time correlation functions can be obtained in closed form, while the purely nuclear correlation functions can be obtained from cavity-free models. In other words, cavity-modified equilibrium FGR rate constants are obtainable from cavity-free inputs.

To further demonstrate the implications of the separability between nuclear and photonic time correlation functions, we will henceforth focus on the relatively simple case where the two-state molecular system is coupled to a single cavity mode. The photonic Hamiltonian for a single-cavity mode is given by

$$\hat{H}^{P} = \frac{1}{2} (\hat{p}_{P}^{2} + \omega_{P}^{2} \hat{q}_{P}^{2}) \tag{10}$$

where $\omega_{\rm p}$ is the cavity mode angular frequency and $\hat{q}_{\rm p}$ and $\hat{p}_{\rm p}$ are the photonic coordinate and momentum operators associated with it, respectively. Assuming that the molecular system is placed at the center of a 1D cavity of length L, with its donor—acceptor transition dipole along the cavity field, the photonic-electronic coupling term is given by 40,41,50

$$\hat{V}_{\mathrm{DA}}^{\mathrm{p}} = \sqrt{2\hbar\omega_{\mathrm{p}}}g_{\mathrm{p}}\hat{q}_{\mathrm{p}} \tag{11}$$

where

$$g_{p} = \sqrt{\frac{\mu_{DA}^{2}\omega_{p}}{2\hbar\varepsilon_{0}V}} \tag{12}$$

Here, $\omega_{\rm p}=c\pi/L$, $\mu_{\rm DA}$ is the donor—acceptor transition dipole moment (assumed to be independent of the nuclear coordinates within the Condon approximation), and V is the cavity volume, given by $V=L_xL_yL_z$, where $L_z=L$ is the cavity length, while L_x and L_y are the dimensions of the cavity perpendicular to the cavity axis. We note that our model Hamiltonian does not include a dipole self-interaction term since such a term corresponds to a constant energy shift in the case of a a two-state model of the type considered here, and therefore has no effect on the dynamics. ⁴⁹

Upon substituting \hat{H}^P and \hat{V}_{DA}^P from eqs 10 and 11 into eq 9, it is straightforward to show that the photonic correlations functions in the second and third terms on the right-hand side (R.H.S.) of eq 9 vanish since the expectation value of the position operator is zero for an undisplaced harmonic oscillator. Furthermore, the photonic correlation functions in the first and fourth terms on the R.H.S. of eq 9 can be obtained in closed form and are given by

$$Tr_{p}[\hat{\rho}_{p}^{eq}e^{i\hat{H}^{p}t/\hbar}e^{-i\hat{H}^{p}t/\hbar}] = 1$$
 (13a)

$$\begin{split} &\operatorname{Tr}_{\mathbf{p}}[\hat{\rho}_{\mathbf{p}}^{\mathrm{eq}} \ \mathrm{e}^{\mathrm{i}\hat{H}^{\mathrm{p}}t/\hbar} \ \hat{V}_{\mathrm{DA}}^{\mathrm{p}} \ \mathrm{e}^{-\mathrm{i}\hat{H}^{\mathrm{p}}t/\hbar} \ \hat{V}_{\mathrm{DA}}^{\mathrm{p}}] \\ &= \hbar^{2} g_{\mathbf{p}}^{2} \bigg(\mathrm{coth} \bigg(\frac{1}{2} \beta \hbar \omega_{\mathbf{p}} \bigg) \, \mathrm{cos}(\omega_{\mathbf{p}}t) \, - \, \mathrm{i} \, \mathrm{sin}(\omega_{\mathbf{p}}t) \bigg) \end{split} \tag{13b}$$

Under the Condon approximation, where $\hat{V}_{DA}^{m} \rightarrow V_{DA}^{m}$ (a constant), eq 9 can be further simplified such that

$$C_{\mathrm{D}\to\mathrm{A}}(t) = \left[1 + \frac{\hbar^2 g_{\mathrm{p}}^2}{(V_{\mathrm{DA}}^n)^2} \left(\mathrm{coth} \left(\frac{1}{2} \beta \hbar \omega_{\mathrm{p}} \right) \mathrm{cos}(\omega_{\mathrm{p}} t) \right. \right.$$
$$\left. - \mathrm{i} \, \sin(\omega_{\mathrm{p}} t) \right] C_{\mathrm{D}\to\mathrm{A}}^m(t) \tag{14}$$

Here, $C_{D\to A}^{m}(t)$ is the cavity-free donor-to-acceptor FGR correlation function within the Condon approximation, which is given by the following [see eq 8]:

$$C_{\rm D\to A}^{\rm m}(t) = (V_{\rm DA}^{\rm n})^2 {\rm Tr}_{\rm n} [\hat{\rho}_{{\rm D},n}^{\rm eq} \, {\rm e}^{{\rm i}\hat{H}_{\rm D}^{\rm n}t/\hbar} \, {\rm e}^{-{\rm i}\hat{H}_{\rm A}^{\rm n}t/\hbar}] \tag{15}$$

Substituting eq 14 back into eq 4, the cavity modified equilibrium FGR rate constant can then be written in the following form:

$$k_{\mathrm{D}\to\mathrm{A}} = k_{\mathrm{D}\to\mathrm{A}}^{\mathrm{m}}(0) + \frac{\hbar^{2}g_{\mathrm{p}}^{2}}{2(V_{\mathrm{DA}}^{n})^{2}} \left[\coth\left(\frac{1}{2}\beta\hbar\omega_{\mathrm{p}}\right) - 1 \right]$$

$$k_{\mathrm{D}\to\mathrm{A}}^{\mathrm{m}}(\omega_{\mathrm{p}}) + \frac{\hbar^{2}g_{\mathrm{p}}^{2}}{2(V_{\mathrm{DA}}^{n})^{2}} \left[\coth\left(\frac{1}{2}\beta\hbar\omega_{\mathrm{p}}\right) + 1 \right] k_{\mathrm{D}\to\mathrm{A}}^{\mathrm{m}}(-\omega_{\mathrm{p}})$$
(16)

where

$$k_{\mathrm{D}\to\mathrm{A}}^{\mathrm{m}}(\omega_{\mathrm{p}}) = \frac{1}{\hbar^{2}} \int_{-\infty}^{\infty} \mathrm{d}t \ \mathrm{e}^{\mathrm{i}\omega_{\mathrm{p}}t} \ C_{\mathrm{D}\to\mathrm{A}}^{\mathrm{m}}(t) \tag{17}$$

is proportional to the Fourier transform of the cavity-free FGR correlation function and $k_{\rm D\to A}^{\rm m}(0)\equiv k_{\rm D\to A}^{\rm m}$ corresponds to the cavity-free equilibrium FGR rate constant. It should be noted that $k_{\rm D\to A}^{\rm m}(\omega_{\rm p})$ can also be thought of as the donor-to-acceptor equilibrium FGR rate constant in a system where the donor PES is shifted *upward* in energy by $\hbar\omega_{\rm p}$ (or equivalently, where the acceptor PES is shifted *downward* in energy by $\hbar\omega_{\rm p}$):

$$\begin{split} k_{\mathrm{D}\to\mathrm{A}}^{\mathrm{m}}(\omega_{\mathrm{p}}) &= \\ &\frac{(V_{DA}^{n})^{2}}{\hbar^{2}} \int_{-\infty}^{\infty} \mathrm{d}t \; \frac{\mathrm{Tr}_{\mathrm{n}}[\mathrm{e}^{-\beta(\hat{H}_{D}^{n}+\hbar\omega_{\mathrm{p}})} \; \mathrm{e}^{\mathrm{i}(\hat{H}_{D}^{n}+\hbar\omega_{\mathrm{p}})t/\hbar} \; \mathrm{e}^{-\mathrm{i}\hat{H}_{A}^{n}t/\hbar}]}{\mathrm{Tr}_{\mathrm{n}}[\mathrm{e}^{-\beta(\hat{H}_{D}^{n}+\hbar\omega_{\mathrm{p}})}]} \\ &= \frac{(V_{DA}^{n})^{2}}{\hbar^{2}} \int_{-\infty}^{\infty} \mathrm{d}t \; \frac{\mathrm{Tr}_{\mathrm{n}}[\mathrm{e}^{-\beta\hat{H}_{D}^{n}} \; \mathrm{e}^{\mathrm{i}\hat{H}_{D}^{n}t/\hbar} \; \mathrm{e}^{-\mathrm{i}(\hat{H}_{A}^{n}t-\hbar\omega_{\mathrm{p}})t/\hbar}]}{\mathrm{Tr}_{\mathrm{n}}[\mathrm{e}^{-\beta\hat{H}_{D}^{n}}]} \end{split}$$

Importantly, the second and third terms on the R.H.S. of eq 16, which represent the effect of the cavity on the equilibrium FGR rate constant, are given in terms of cavity-free inputs, namely, $C_{D\to A}^{m}(t)$ [see eq 17].

Further insight into eq 16 can be gained by taking advantage of the detailed balance relation in the cavity-free case, according to which

$$k_{\mathrm{D}\to\mathrm{A}}^{\mathrm{m}}(-\omega_{\mathrm{p}}) = \frac{Z_{\mathrm{A}}^{n}}{Z_{\mathrm{D}}^{n}} \,\mathrm{e}^{-\beta\hbar\omega_{\mathrm{p}}} \,k_{\mathrm{A}\to\mathrm{D}}^{\mathrm{m}}(\omega_{\mathrm{p}}) \tag{19}$$

Here, $Z_D^n = \operatorname{Tr}_n[e^{-\beta \hat{H}_D^n}]$ and $Z_A^n = \operatorname{Tr}_n[e^{-\beta \hat{H}_A^n}]$ are the cavity-free donor and acceptor partition functions, respectively [see eq 6], and

$$k_{\mathrm{A}\to\mathrm{D}}^{\mathrm{m}}(\omega_{\mathrm{p}}) = \frac{1}{\hbar^{2}} \int_{-\infty}^{\infty} \mathrm{d}t \ \mathrm{e}^{\mathrm{i}\omega_{\mathrm{p}}t} \ C_{\mathrm{A}\to\mathrm{D}}^{\mathrm{m}}(t) \tag{20}$$

is proportional to the Fourier transform of the cavity-free *acceptor-to-donor* FGR correlation function, which (within the Condon approximation) is given by

$$C_{A\to D}^{m}(t) = (V_{DA}^{n})^{2} \operatorname{Tr}_{n} [\hat{\rho}_{A,n}^{eq} e^{i\hat{H}_{A}^{n}t/\hbar} e^{-i\hat{H}_{D}^{n}t/\hbar}]$$
(21)

Here, $\hat{\rho}_{A,n}^{eq}=\mathrm{e}^{-\beta\hat{H}_A^n}/Z_A^n$. It should be noted that $k_{\mathrm{A}\to\mathrm{D}}^{\mathrm{m}}(0)\equiv k_{\mathrm{A}\to\mathrm{D}}^{\mathrm{m}}$ corresponds to the cavity-free acceptor-to-donor equilibrium FGR rate constant (not to be confused with the cavity-free donor-to-acceptor equilibrium FGR rate constant [see eqs 15 and 21]. It should also be noted that $k_{\mathrm{A}\to\mathrm{D}}^{\mathrm{m}}(\omega_{\mathrm{p}})$ can also be thought of as the acceptor-to-donor equilibrium FGR rate constant in a system where the donor PES is shifted downward in energy by $\hbar\omega_{\mathrm{p}}$ (or equivalently, where the acceptor PES is shifted upward in energy by $\hbar\omega_{\mathrm{p}}$):

$$\begin{split} k_{\mathrm{A}\to\mathrm{D}}^{\mathrm{m}}(\omega_{\mathrm{p}}) &= \\ &\frac{(V_{DA}^{n})^{2}}{\hbar^{2}} \int_{-\infty}^{\infty} \mathrm{d}t \; \frac{\mathrm{Tr}_{\mathrm{n}}[\mathrm{e}^{-\beta(\hat{H}_{A}^{n}+\hbar\omega_{\mathrm{p}})}\,\mathrm{e}^{\mathrm{i}(\hat{H}_{A}^{n}+\hbar\omega_{\mathrm{p}})t/\hbar}\,\,\mathrm{e}^{-\mathrm{i}\hat{H}_{D}^{n}t/\hbar}]}{\mathrm{Tr}_{\mathrm{n}}[\mathrm{e}^{-\beta(\hat{H}_{A}^{m}+\hbar\omega_{\mathrm{p}})}]} \\ &= \frac{V_{DA}^{2}}{\hbar^{2}} \int_{-\infty}^{\infty} \mathrm{d}t \; \frac{\mathrm{Tr}_{\mathrm{n}}[\mathrm{e}^{-\beta\hat{H}_{A}^{n}}\,\mathrm{e}^{\mathrm{i}\hat{H}_{A}^{n}t/\hbar}\,\,\mathrm{e}^{-\mathrm{i}(\hat{H}_{D}^{n}-\hbar\omega_{\mathrm{p}})t/\hbar}]}{\mathrm{Tr}_{\mathrm{n}}[\mathrm{e}^{-\beta\hat{H}_{A}^{n}}]} \end{split}$$
(22)

Substituting eq 19 for $k_{\rm D\to A}^{\rm m}(-\omega_{\rm p})$ into eq 16, eq 16 can be recast in the following form:

$$\frac{k_{\mathrm{D}\to\mathrm{A}}}{k_{\mathrm{D}\to\mathrm{A}}^{\mathrm{m}}} - 1 = \frac{\hbar^2 g_{\mathrm{p}}^2}{(V_{\mathrm{DA}}^n)^2} \langle \hat{N}(\beta \hbar \omega_{\mathrm{p}}) \rangle_{\mathrm{eq}} \left[\frac{k_{\mathrm{D}\to\mathrm{A}}^{\mathrm{m}}(\omega_{\mathrm{p}})}{k_{\mathrm{D}\to\mathrm{A}}^{\mathrm{m}}(0)} + \frac{k_{\mathrm{A}\to\mathrm{D}}^{\mathrm{m}}(\omega_{\mathrm{p}})}{k_{\mathrm{A}\to\mathrm{D}}^{\mathrm{m}}(0)} \right]$$
(23)

Here

$$\langle \hat{N}(\beta\hbar\omega_{\rm p})\rangle_{\rm eq} = \frac{1}{{\rm e}^{\beta\hbar\omega_{\rm p}} - 1} \tag{24}$$

is the expectation value of the number of photons in the cavity mode at thermal equilibrium. Importantly, $k_{\rm D\to A}\to k_{\rm D\to A}^{\rm m}$, and therefore $\frac{k_{\rm D\to A}}{k_{\rm D\to A}^{\rm m}}-\vec{1}\to 0$ in the cavity-free case. Thus, the R.H.S. of eq 23 represents the effect of the cavity on the donor-to-acceptor equilibrium FGR rate constant. It should also be noted that since the R.H.S. of eq 23 is non-negative for this particular model, placing the molecular system inside the cavity will always result in enhancement of the donor-to-acceptor equilibrium FGR rate constant (i.e., $k_{\rm D\to A}>k_{\rm D\to A}^{\rm m}$).

Inspection of the R.H.S. of eq 23 reveals that it consists of a product of three dimensionless factors, namely, $(1) \frac{\hbar^2 g_p^2}{(V_{\rm DM}^{\rm m})^2}$, $(2) \langle \hat{N}(\beta\hbar\omega_p)\rangle_{\rm eq}$, and $(3) \left[\frac{k_{\rm D-A}^{\rm m}(\omega_p)}{k_{\rm D-A}^{\rm m}(0)} + \frac{k_{\rm A-D}^{\rm m}(\omega_p)}{k_{\rm A-D}^{\rm m}(0)}\right]$. A reasonable criterion for when a significant cavity-induced enhancement of the donor-to-acceptor equilibrium FGR rate constant would be achieved is when this triple product is larger than 1 (i.e., $\frac{k_{\rm D-A}}{k_{\rm D-A}^{\rm m}} - 1 \geq 1$). This is because $\frac{k_{\rm D-A}}{k_{\rm D-A}^{\rm m}} - 1 = 1$ implies $\frac{k_{\rm D-A}}{k_{\rm D-A}^{\rm m}} = 2$, which means that the electronic transition rate constant would double upon placing the molecular system

inside a cavity. Thus, requiring that $\frac{k_{\rm D\to A}}{k_{\rm D\to A}^{\rm m}}-1\geq 1$ means enhancing the rate constant by a factor of 2 or more.

Of particular interest is the dependence of the aforementioned triple product on the cavity mode frequency $\omega_{\rm p}$, which is often used experimentally to tune the cavity in a manner that would optimize its effect on the rate constant of the chemical process under consideration. To this end, we will consider below the $\omega_{\rm p}$ dependence of each factor separately.

The first factor, $\frac{\hbar^2 g_{\rm p}^2}{(V_{\rm DA}^n)^2}$, consists of the ratio of the radiative and nonradiative electronic coupling strengths. It should be noted that FGR relies on treating both types of electronic coupling as small enough for second-order perturbation theory to be applicable. Thus, a significant rate enhancement only requires that the cavity-induced coupling strength, $\hbar^2 g_{\rm p}^2$, is comparable to the already presumably relatively weak nonradiative electronic coupling strength, $(V_{\rm DA}^n)^2$, so that $\frac{\hbar^2 g_{\rm p}^2}{(V_{\rm DA}^n)^2} \sim 1$. Using eq 12 and the fact that $\omega_{\rm p} = c\pi/L$, this factor can also be cast in the following form:

$$\frac{\hbar^2 g_{\rm p}^2}{(V_{\rm DA}^{\rm m})^2} = \frac{1}{\chi} (\beta \hbar \omega_{\rm p})^2$$
 (25)

where χ is a molecule- and cavity-specific dimensionless quantity given by

$$\chi = 2\pi c \varepsilon_0 \hbar L_x L_y \left(\frac{\beta V_{DA}^n}{\mu_{DA}} \right)^2 \tag{26}$$

Here, L_x and L_y are the dimensions of the cavity perpendicular to the cavity axis which is assumed to coincide with the z axis, such that the cavity volume is given by $V = L_x L_y L_z$ where $L_z = L$ is the cavity length. Importantly, $g_p^2 \propto \omega_p^2$, regardless of the specific nature of the molecular system, which means that this term monotonically increases with increasing cavity mode frequency in a manner that *is not* molecular-system-specific.

frequency in a manner that is not molecular-system-specific. The second factor, $\langle \hat{N}(\beta\hbar\omega_{\rm p})\rangle_{\rm eq}=\frac{1}{e^{i\hbar\omega_{\rm p}}-1}$, corresponds to the expectation value of the number of photons in the cavity mode at thermal equilibrium. It should be noted that this factor increases with increasing temperature, $T=(k_{\rm B}\beta)^{-1}$, and vanishes at T=0, which means that rate enhancement does not occur in the dark (i.e., at T=0). It should also be noted that $\langle \hat{N}(\beta\hbar\omega_{\rm p})\rangle_{\rm eq}$ decreases with increasing cavity mode frequency, $\omega_{\rm p}$, in a manner which is not molecular-system-specific. The fact that the first factor is a monotonically increasing quadratic function of $\omega_{\rm p}$, while the second factor is asymptotically a monotonically decreasing exponential function of $\omega_{\rm p}$ also suggests that the product of these two factors would be maximized at a finite value of $\omega_{\rm p}$.

Unlike the first two factors, the third factor, $\left[\frac{k_{\mathrm{D-A}}^{\mathrm{m}}(\omega_{\mathrm{p}})}{k_{\mathrm{D-A}}^{\mathrm{m}}(0)} + \frac{k_{\mathrm{A-D}}^{\mathrm{m}}(\omega_{\mathrm{p}})}{k_{\mathrm{A-D}}^{\mathrm{m}}(0)}\right]$, is molecular-system-specific and understanding its dependence on ω_{p} and T calls for explicit expressions for $k_{\mathrm{D-A}}^{\mathrm{m}}(\omega_{\mathrm{p}})$ and $k_{\mathrm{A-D}}^{\mathrm{m}}(\omega_{\mathrm{p}})$, within an FGR-based rate theory of one's choice. In the next section, we demonstrate this within the framework of Marcus theory.

3. RESULTS AND DISCUSSION

The equilibrium FGR rate constant reduces to the Marcus theory rate constant when the correlation function is replaced by its short-time and high temperature limits and nuclear dynamics are assumed to satisfy Gaussian statistics.^{69,70} Within Marcus theory, one can obtain the following closed form expressions for $k_{D\rightarrow A}^{m}(0)$, $k_{A\rightarrow D}^{m}(0)$, $k_{D\rightarrow A}^{m}(\omega_{p})$, and $k_{A\rightarrow D}^{m}(\omega_{p})$:⁶⁹

$$k_{\rm D\to A}^{\rm m}(0) = \frac{(V_{DA}^m)^2}{\hbar} \sqrt{\frac{\pi}{k_{\rm B}TE_r}} e^{-(\Delta E + E_r)^2/4k_{\rm B}TE_r}$$
 (27)

$$k_{\rm A \to D}^{\rm m}(0) = \frac{(V_{DA}^m)^2}{\hbar} \sqrt{\frac{\pi}{k_{\rm B} T E_r}} e^{-(-\Delta E + E_r)^2 / 4k_{\rm B} T E_r}$$
 (28)

$$k_{\rm D\to A}^{\rm m}(\omega_{\rm p}) = \frac{(V_{DA}^{m})^2}{\hbar} \sqrt{\frac{\pi}{k_{\rm B}TE_{\rm r}}} e^{-(\Delta E - \hbar\omega_{\rm p} + E_{\rm r})^2/4k_{\rm B}TE_{\rm r}}$$
 (29)

$$k_{\mathrm{A}\to\mathrm{D}}^{\mathrm{m}}(\omega_{\mathrm{p}}) = \frac{(V_{DA}^{m})^{2}}{\hbar} \sqrt{\frac{\pi}{k_{\mathrm{B}}TE_{r}}} \, \mathrm{e}^{-(-\Delta E - \hbar\omega_{\mathrm{p}} + E_{r})^{2}/4k_{\mathrm{B}}TE_{r}}$$
(30)

Here, ΔE is the cavity-free donor-to-acceptor reaction free energy and E_r is the cavity-free reorganization energy. In what follows, we will assume that the cavity-free donor-to-acceptor transition is thermodynamically favorable (i.e., that the donor-to-acceptor transition is a downhill reaction), such that $\Delta E < 0$. It should be noted that as a result, the cavity-free acceptor-to-donor reaction energy is positive and given by $-\Delta E > 0$ (an uphill reaction).

Of particular interest is the dependence of the third factor on the R.H.S. of eq 23, $\left[\frac{k_{\rm D\rightarrow A}^{\rm m}(\omega_{\rm p})}{k_{\rm D\rightarrow A}^{\rm m}(0)}+\frac{k_{\rm A\rightarrow D}^{\rm m}(\omega_{\rm p})}{k_{\rm A\rightarrow D}^{\rm m}(0)}\right]$, on $\omega_{\rm p}$, since the cavity-induced effect is often optimized by tuning ω_p . We start out by considering the first ratio, $\frac{k_{\rm D-A}^{\rm m}(\omega_{\rm p})}{k_{\rm D-A}^{\rm m}(0)}$. Comparing eqs 27 and 29, we see that while $k_{\rm D\to A}^{\rm m}(0)$ corresponds to the actual cavity-free donor-to-acceptor Marcus rate constant in the case when the reaction energy is ΔE , $k_{\mathrm{D} \to \mathrm{A}}^{\mathrm{m}}(\omega_{\mathrm{p}})$ corresponds to what that rate constant would have been if the reaction energy was $\Delta E - \hbar \omega_p$ (see Figure 1). Given that $\Delta E < 0$, increasing $\omega_{\rm p}$ corresponds to making the reaction energy more negative. If the actual cavity-free reaction is in the normal Marcus regime $(-\Delta E < E_r)$, as in Figure 1), then $\frac{k_{\rm D\to A}^{\rm m}(\omega_{\rm p})}{k_{\rm D\to A}^{\rm m}(0)}$ would exhibit a nonmonotonic dependence on $\omega_{\rm p}$, namely, it would increase with increasing ω_p within $0 < \omega_p < (\Delta E + E_r)/\hbar$ and decrease with increasing $\omega_{\rm p}^{\rm F}$ for $\omega_{\rm p} > (\Delta E + E_{\rm r})/\hbar$ (see Figure 1). If, on the other hand, the actual cavity-free reaction is in the inverted Marcus regime $(-\Delta E > E_r)$, then $\frac{k_{\rm D-A}^{\rm m}(\omega_{\rm p})}{k_{\rm D-A}^{\rm m}(0)}$ would monotonically decrease with increasing $\omega_{\rm p}$. Thus, $\frac{k_{\rm D-A}^{\rm m}(\omega_{\rm p})}{k_{\rm D-A}^{\rm m}(0)}>1$ only if the cavity-free donor-to-acceptor reaction is in the normal regime and even then on a relatively narrow ω_p range $0 < \omega_p <$ $2(\Delta E + E_r)/\hbar$ and giving rise to relatively small rate enhancement. We acknowledge that for sufficiently high values of $\hbar\omega_{\rm n}$, excitations to higher lying electronic states may become relevant. While the analysis presented herein is based

on assuming that the molecular system can be described in terms of a two-state model, it can be extended to include

additional electronic states. Work on this aspect is ongoing and

will be presented in forthcoming publications.

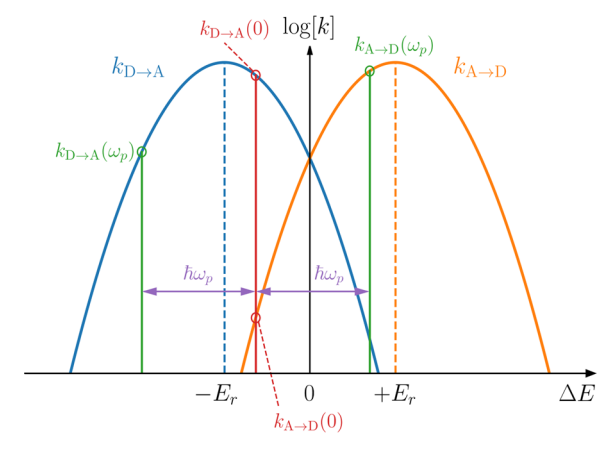


Figure 1. Schematic view of the various Marcus rate constants in eqs 27–30. The dependence of $k_{D\to A}$ (blue) and $k_{A\to D}$ (orange) on ΔE is shown on a semilog plot. $k_{D\to A}(0)$ and $k_{A\to D}(0)$ correspond to the cavity-free rate constants (for the case where $\Delta E < 0$ and the donor-to-acceptor reaction is in the normal region). $k_{D\to A}(\omega_p)$ and $k_{A\to D}(\omega_p)$ are the corresponding rate constants when the donor potential energy surface is shifted upward or downward by $\hbar \omega_{p}$, respectively.

Next, consider the second ratio, $\frac{k_{A-D}^m(\omega_p)}{k_{A-D}^m(0)}$. Comparing eqs 28 and 30, we see that while $k_{A\to D}^{m}(0)$ corresponds to the actual acceptor-to-donor cavity-free Marcus rate constant in the case when the reaction energy is $-\Delta E$, $k_{A\to D}^{m}(\omega_{p})$ corresponds to what the rate constant would have been if the reaction energy was $-\Delta E - \hbar \omega_p$. Importantly, the actual cavity-free acceptorto-donor reaction rate constant, $k_{A\to D}^{m}(0)$, would typically be vanishingly small since $-\Delta E > 0$ (see Figure 1). Increasing $\omega_{\rm p}$ therefore lowers the reaction energy by making it less positive, and eventually negative, which would typically lead to a considerable rate enhancement which is maximized when $\omega_{\rm p}$ = $(-\Delta E + E_r)/\hbar$ (see Figure 1). Increasing ω_p beyond this point would decrease $k_{A\to D}^{m}(\omega_{p})$. However, it should be noted that $\frac{k_{\rm A\to D}^{\rm m}(\omega_{\rm p})}{k_{\rm A\to D}^{\rm m}(0)}>1$ on a relatively wide $\omega_{\rm p}$ range, 0 < $\omega_{\rm p}<2(-\Delta E+$ $(E_r)/\hbar$, and that the $\frac{k_{A\to D}^{\rm m}(\omega_p)}{k_{A\to D}^{\rm m}(0)}$ term gives rise to a much larger rate enhancement in comparison to the $\frac{k_{\rm D\to A}^{\rm m}(\omega_{\rm p})}{k_{\rm D\to A}^{\rm m}(0)}$ term (given that $\Delta E \leq 0$ and $E_r > 0$, it follows that $k_{\rm A\to D}^{\rm m}(\omega_{\rm p})/k_{\rm A\to D}^{\rm m}(0) \geq k_{\rm D\to A}^{\rm m}(\omega_{\rm p})/k_{\rm D\to A}^{\rm m}(0) \text{, with equality at}$ $\omega_{\rm p}$ = 0). Thus, the cavity-induced rate enhancement would typically be dominated by the term $\frac{k_{n-p}^{\text{M}}(\omega_p)}{k_{n-p}^{\text{M}}(0)}$ rather than the term $\frac{k_{\rm D\to A}^{\rm m}(\omega_{\rm p})}{k_{\rm D\to A}^{\rm m}(0)}$.

Substituting eqs 24 and 25 into eq 23, one can cast the inequality $\frac{k_{\rm D-A}}{k_{\rm m}^{\rm m}} - 1 \ge 1$ in the following form:

$$\frac{1}{G(\beta\hbar\omega_{\rm p})} \left[\frac{k_{\rm D\to A}^{\rm m}(\omega_{\rm p})}{k_{\rm D\to A}^{\rm m}(0)} + \frac{k_{\rm A\to D}^{\rm m}(\omega_{\rm p})}{k_{\rm A\to D}^{\rm m}(0)} \right] \ge 1 \tag{31}$$

where

$$G(\beta\hbar\omega_{\rm p}) = \frac{1}{\chi} \frac{e^{\beta\hbar\omega_{\rm p}} - 1}{(\beta\hbar\omega_{\rm p})^2}$$
(32)

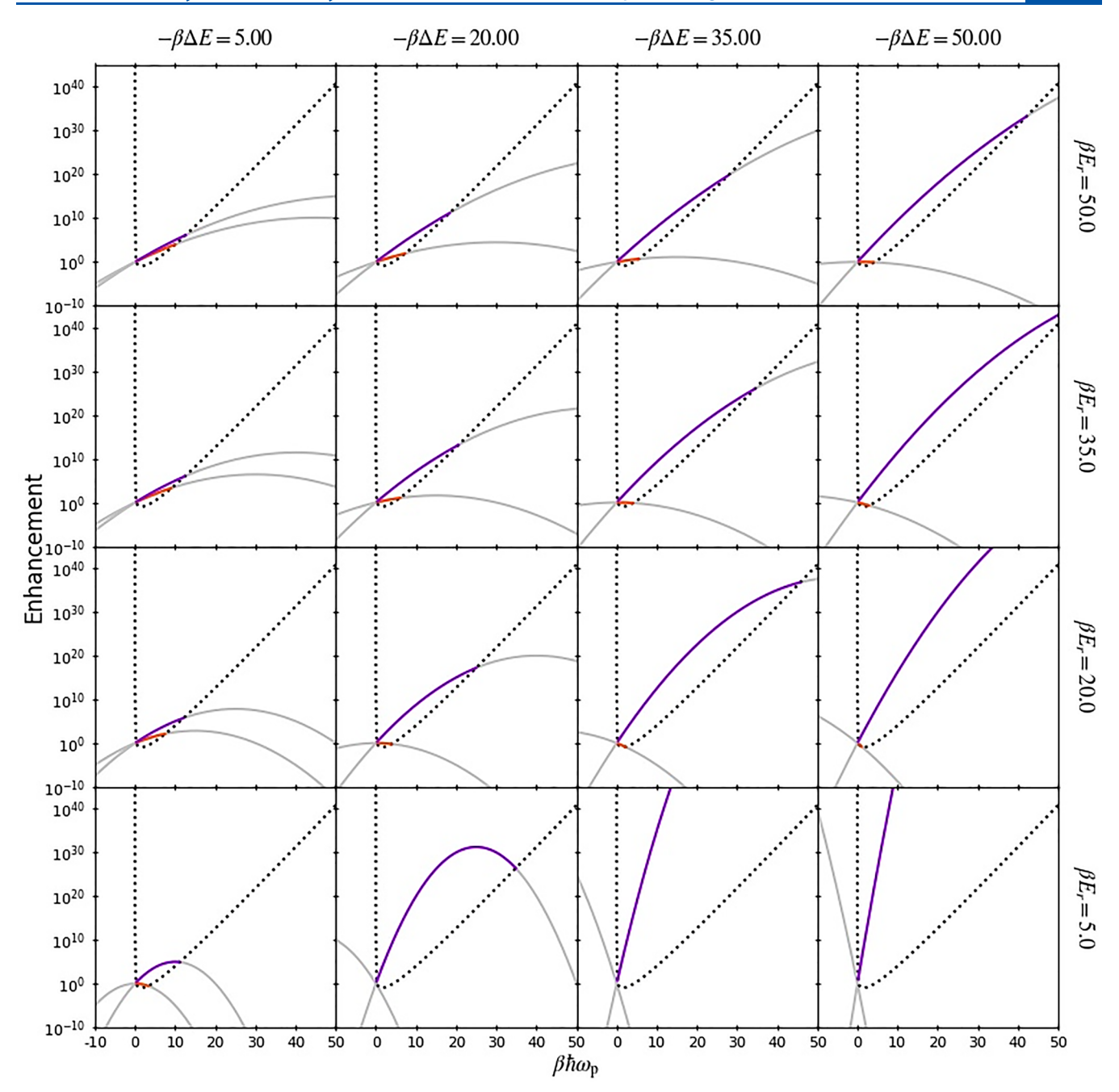


Figure 2. $G(\beta\hbar\omega_{\rm p})$ (dashed black line), $\frac{k_{\rm D\to A}^{\rm m}(\omega_{\rm p})}{k_{\rm D\to A}^{\rm m}(0)}$ and $\frac{k_{\rm A\to D}^{\rm m}(\omega_{\rm p})}{k_{\rm A\to D}^{\rm m}(0)}$ (solid gray lines), as a function of $\beta\hbar\omega_{\rm p}$, for different values of ΔE and E_r . The intervals within which $\frac{k_{\rm D\to A}^{\rm m}(\omega_{\rm p})}{k_{\rm D\to A}^{\rm m}(0)} \geq G(\beta\hbar\omega_{\rm p})$ (red) and $\frac{k_{\rm A\to D}^{\rm m}(\omega_{\rm p})}{k_{\rm A\to D}^{\rm m}(0)} \geq G(\beta\hbar\omega_{\rm p})$ (purple) correspond to the range of $\omega_{\rm p}$ values for which each of those terms can give rise to cavity-induced rate enhancement.

Assuming that Marcus theory is valid, the ratios $\frac{k_{\rm D-A}^{\rm m}(\omega_{\rm p})}{k_{\rm D-A}^{\rm m}(0)}$ and

 $\frac{k_{\rm A \to D}^{\rm m}(\omega_{\rm p})}{k_{\rm A \to D}^{\rm m}(0)}$ are given by [see eqs 27–30]:

$$\frac{k_{\mathrm{D}\to\mathrm{A}}^{\mathrm{m}}(\omega_{\mathrm{p}})}{k_{\mathrm{D}\to\mathrm{A}}^{\mathrm{m}}(0)} = \exp\left[-\frac{(\beta\hbar\omega_{\mathrm{p}})^{2} - 2\beta\hbar\omega_{\mathrm{p}}(\beta\Delta E + \beta E_{r})}{4\beta E_{r}}\right]$$
(33)

$$\frac{k_{\rm A\to D}^{\rm m}(\omega_{\rm p})}{k_{\rm A\to D}^{\rm m}(0)} = \exp\left[-\frac{(\beta\hbar\omega_{\rm p})^2 - 2\beta\hbar\omega_{\rm p}(-\beta\Delta E + \beta E_{\rm r})}{4\beta E_{\rm r}}\right]$$
(34)

A useful graphical depiction of the implications of eq 31 can be obtained by plotting $G(\beta\hbar\omega_{\rm p}), \frac{k_{\rm D-A}^{\rm m}(\omega_{\rm p})}{k_{\rm D-A}^{\rm m}(0)}$, and $\frac{k_{\rm A-D}^{\rm m}(\omega_{\rm p})}{k_{\rm A-D}^{\rm m}(0)}$ as a function of $\beta\hbar\omega_{\rm p}$. As shown in Figure 2, the intervals within which $\frac{k_{\rm D-A}^{\rm m}(\omega_{\rm p})}{k_{\rm D-A}^{\rm m}(0)} \geq G(\beta\hbar\omega_{\rm p})$ and $\frac{k_{\rm A-D}^{\rm m}(\omega_{\rm p})}{k_{\rm A-D}^{\rm m}(0)} \geq G(\beta\hbar\omega_{\rm p})$ correspond to the range of $\omega_{\rm p}$ values for which each of those terms can give rise to cavity-induced rate enhancement. Inspection of

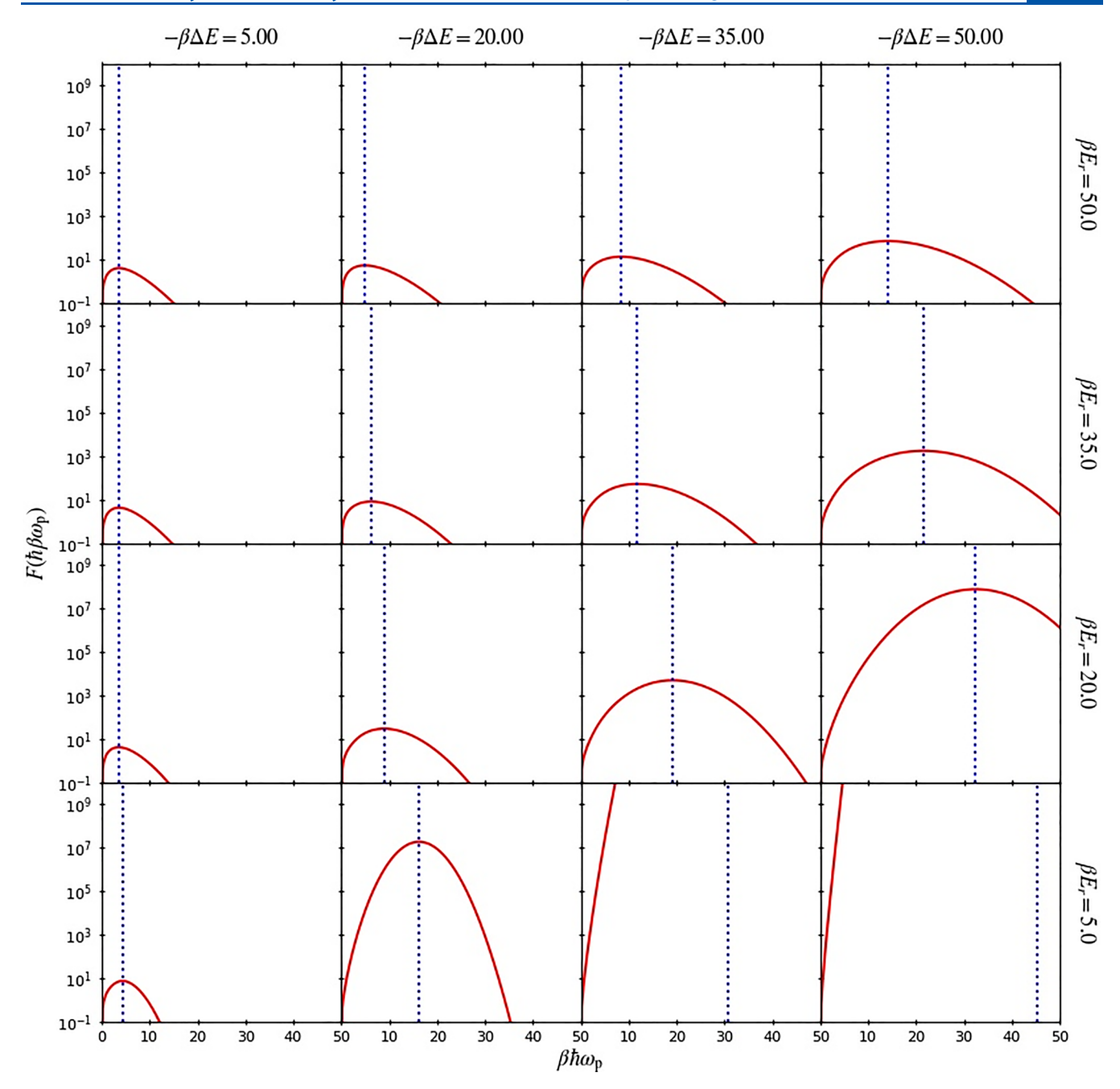


Figure 3. Plots of $F[\beta\hbar\omega_p; \beta\Delta E, \beta E_r]$ [see eq 36], as a function of $\beta\hbar\omega_p$ for different values of $\beta\Delta E$ and βE_r . The vertical dotted line marks the cavity frequency at which $F[\beta\hbar\omega_p; \beta\Delta E, \beta E_r]$ is maximized.

Figure 2 confirms that the rate-enhancement is dominated by the $\frac{k_{\mathrm{D}\to\mathrm{A}}^{\mathrm{m}}(\omega_{\mathrm{p}})}{k_{\mathrm{A}\to\mathrm{D}}^{\mathrm{m}}(0)}$ term, rather than the $\frac{k_{\mathrm{D}\to\mathrm{A}}^{\mathrm{m}}(\omega_{\mathrm{p}})}{k_{\mathrm{D}\to\mathrm{A}}^{\mathrm{m}}(0)}$ term, both in terms of the range of ω_{p} interval within which rate enhancement is achieved and in terms of the actual enhancement. This trend is also seen to become more pronounced with increasing $|\Delta E|$ and decreasing E_r (see below).

Importantly, the minimum of $G(\beta\hbar\omega_{\rm p})$ is at $\beta\hbar\omega_{\rm p}\approx 1.6$, independent of the molecular system, which corresponds to $\hbar\omega_{\rm p}\sim 0.04$ eV at room temperature. At the same time, typical values of ΔE and E_r correspond to $\beta|\Delta E|\gg 1$ and $\beta E_r\gg 1$ at room temperature. For example, the 5.0–50.0 range of $\beta|\Delta E|$ and βE_r used in Figure 2 corresponds to a typical range of $(0.13-1.30){\rm eV}$ for $|\Delta E|$ and E_r at room temperature. One therefore expects the maximum overall enhancement would be

achieved somewhere between $\beta\hbar\omega_{\rm p}=1.6$ and $\beta\hbar\omega_{\rm p}=\beta E_r-\beta\Delta E$, the latter being the maximum point of the $\frac{k_{\rm A\to D}^{\rm m}(\omega_{\rm p})}{k_{\rm A\to D}^{\rm m}(0)}$ term.

Further insight can be obtained by using eqs 33 and 34 to cast the molecular-system-specific third factor on the R.H.S. of

eq 23,
$$\left[\frac{k_{\mathrm{D}\to\mathrm{A}}^{\mathrm{m}}(\omega_{\mathrm{p}})}{k_{\mathrm{D}\to\mathrm{A}}^{\mathrm{m}}(0)} + \frac{k_{\mathrm{A}\to\mathrm{D}}^{\mathrm{m}}(\omega_{\mathrm{p}})}{k_{\mathrm{A}\to\mathrm{D}}^{\mathrm{m}}(0)}\right]$$
, in the following form:

$$\begin{split} & \left[\frac{k_{\mathrm{D}\to\mathrm{A}}^{\mathrm{m}}(\omega_{\mathrm{p}})}{k_{\mathrm{D}\to\mathrm{A}}^{\mathrm{m}}(0)} + \frac{k_{\mathrm{A}\to\mathrm{D}}^{\mathrm{m}}(\omega_{\mathrm{p}})}{k_{\mathrm{A}\to\mathrm{D}}^{\mathrm{m}}(0)} \right] \\ & = 2 \, \mathrm{e}^{-(\beta\hbar\omega_{\mathrm{p}})^{2} - 2(\beta\hbar\omega_{\mathrm{p}})(\beta E_{r})/4(\beta E_{r})} \cosh \left[\frac{(\beta\Delta E)(\beta\hbar\omega_{\mathrm{p}})}{2(\beta E_{r})} \right] \end{split}$$

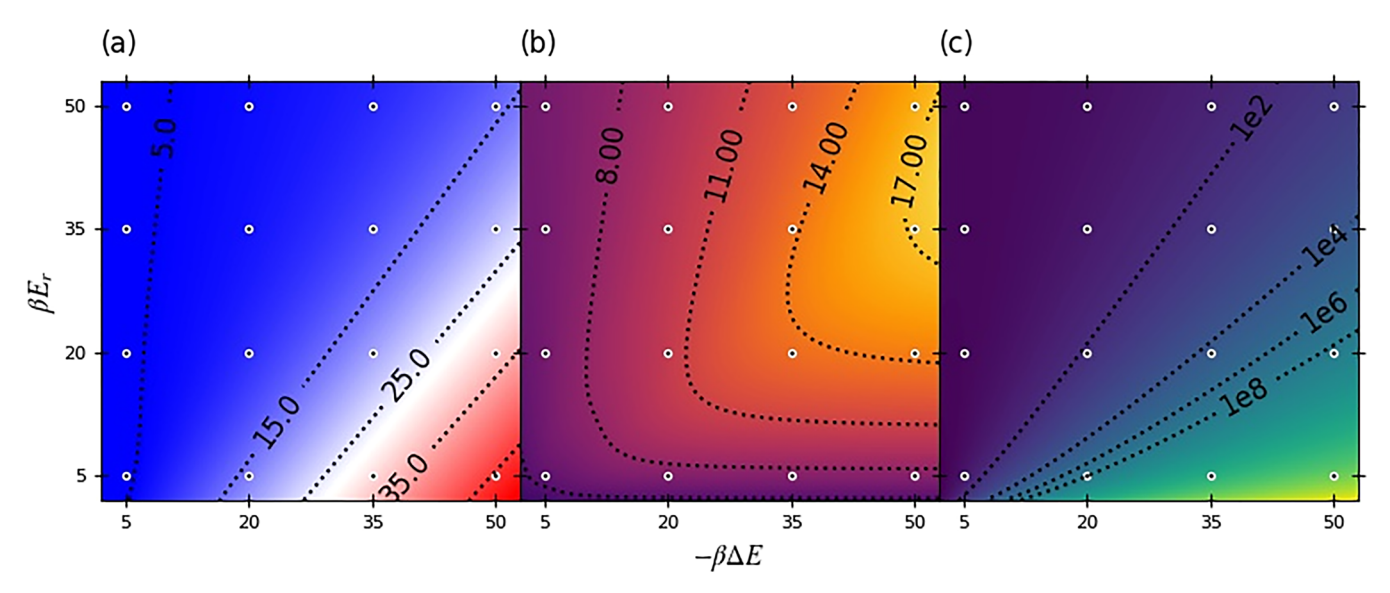


Figure 4. (a) Optimal cavity frequency $\beta\hbar\omega_{\rm p}$, $\beta\hbar\omega_{\rm max}$, as a function of $-\beta\Delta E$ and βE_r . (b) FWHM of $F(\beta\hbar\omega_{\rm p})$, as a function of $\beta\Delta E$ and βE_r . (c) Maximal value of $F(\beta\hbar\omega_{\rm p})$, $F(\beta\hbar\omega_{\rm max})$, as a function of $\beta\Delta E$ and βE_r . βE_r and $\beta\Delta E$ corresponding to the panels of Figures 2, 3 are shown as black dots on the plot.

Substituting eqs 24, 25, and 35 back into eq 23, the criterion for more than double cavity-induced rate enhancement, $\frac{k_{\rm D-A}}{k_{\rm D-A}^{\rm m}}-1\geq 1$, can be written in the following form:

$$\begin{split} F[\beta\hbar\omega_{\rm p};\,\beta\Delta E,\,\beta E_{\rm r}] &\equiv \frac{2(\beta\hbar\omega_{\rm p})^2}{{\rm e}^{\beta\hbar\omega_{\rm p}}-1}\,\,{\rm e}^{-(\beta\hbar\omega_{\rm p})^2-2(\beta\hbar\omega_{\rm p})(\beta E_{\rm r})/4(\beta E_{\rm r})}\\ &\cosh\!\left[\frac{(\beta\Delta E)(\beta\hbar\omega_{\rm p})}{2(\beta E_{\rm r})}\right] &\geq \chi \end{split} \tag{36}$$

The usefulness of eq 36 comes from the fact that calculating $F[\beta\hbar\omega_{\rm p};\,\beta\Delta E,\,\beta E_{\rm r}]$ on its left-hand side (L.H.S.) only requires knwlegede of the cavity-free parameters ΔE and E_n temperature, T, and the cavity mode frequency, ω_p , while the parameter χ on its R.H.S. is given in terms of cavity-free molecular transition dipole, μ_{DA} , the electronic coupling coefficient in units of k_BT , βV_{DA}^n , and the cavity transverse dimensions L_x and L_y [see eq 26]. As such, it can be used to optimize the cavity-induced rate enhancement for any system whose cavity-free kinetics is described by Marcus theory. More specifically, given T and the cavity-free ΔE and E_r for the electronic charge/energy transfer reaction under consideration, one can maximize $F[\beta\hbar\omega_{\rm p};\,\beta\Delta E,\,\beta E_{\rm r}]$ with respect to the cavity mode frequency, $\omega_{\rm p}$. Furthermore, the fact that all relevant energies (ΔE , E_r , V_{DA}^n , and $\hbar \omega_{\rm p}$) are given in units of $k_{\rm B}T$ (i.e., as $\beta\Delta E$, $\beta E_{\rm r}$, $\beta V_{\rm DA}^n$ and $\beta\hbar\omega_{\rm p}$, respectively) implies that the temperature dependence corresponds to an energy scaling factor.

In Figure 3, we show plots of $F[\beta\hbar\omega_{\rm p};\beta\Delta E,\beta E_{\rm r}]$ as a function of $\beta\hbar\omega_{\rm p}$ for different values of $-\beta\Delta E$ and $\beta E_{\rm r}$, and the corresponding values of $\beta\hbar\omega_{\rm p}$ at which $F[\beta\hbar\omega_{\rm p};\beta\Delta E,\beta E_{\rm r}]$ is maximized.

Further analysis is shown in Figure 4, which depicts the optimal cavity frequency $\beta\hbar\omega_{max}$ [Figure 4(a)], the full width at half maximum (FWHM) of $F(\beta\hbar\omega_p)$ [panel (b)] and the maximal value of $F(\beta\hbar\omega_p)$, $F(\beta\hbar\omega_{max})$ [Figure 4(c)], as a function of $-\beta\Delta E$ and βE_r .

Several interesting observations can be discerned based on these figures:

- $F[\beta\hbar\omega_p; \beta\Delta E, \beta E_r]$ has a single maximum as a function of $\beta\hbar\omega_p$. Thus, $F[\beta\hbar\omega_p; \beta\Delta E, \beta E_r]$, and thereby the cavity-induced rate enhancement, can clearly be maximized by optimizing ω_p .
- Given βE_n both $\beta \hbar \omega_{max}$ and $F(\beta \hbar \omega_{max})$ increase with increasing $|\Delta E|$, [see Figure 4(a,c)]. This is consistent with the fact that increasing $|\Delta E|$ enhances $\frac{k_{\rm A-D}^{\rm m}(\omega_{\rm p})}{k_{\rm A-D}^{\rm m}(0)}$ and shifts it to higher values of $\beta \hbar \omega_{\rm p}$ (see Figure 2).
- Given $\beta\Delta E$, both $\beta\hbar\omega_{\rm max}$ and $F(\beta\hbar\omega_{\rm max})$ increase with decreasing E_r [see Figure 4(a,c)]. This is consistent with the behavior of $\frac{k_{\rm A-D}^m(\omega_{\rm p})}{k_{\rm A-D}^m(0)}$ in Figure 2 where it is seen to be enhanced and to narrow down (as a function of $\beta\hbar\omega_{\rm p}$) with decreasing E_r . Analysis of eq 34 confirms that $\frac{k_{\rm A-D}^m(\omega_{\rm p})}{k_{\rm A-D}^m(0)}$ increases with decreasing E_r within a relatively wide interval of $\omega_{\rm p}$ values, $0 < \hbar\omega_{\rm p} < -2\Delta E$ (i.e., $\frac{d}{dE_r}\frac{k_{\rm A-D}^m(\omega_{\rm p})}{k_{\rm A-D}^m(0)} < 0$ within this range). Importantly, the optimal values of $\omega_{\rm p}$ fall within this range for the typical values of βE_r and $\beta \Delta E$ used in Figures 3 and 4. It should be noted that the value of $\omega_{\rm p}$ for which $\frac{k_{\rm A-D}^m(\omega_{\rm p})}{k_{\rm A-D}^m(0)}$ is maximized is given by $\hbar\omega_{\rm p} = E_r \Delta E$, which actually decreases with decreasing E_r . However, the condition $\frac{k_{\rm A-D}^m(\omega_{\rm p})}{k_{\rm A-D}^m(\omega_{\rm p})} \geq G(\beta\hbar\omega_{\rm p})$ means that the actual maximum of $F[\beta\hbar\omega_{\rm p}; \beta\Delta E, \beta E_r]$ falls in the region where $\frac{k_{\rm A-D}^m(\omega_{\rm p})}{k_{\rm A-D}^m(0)}$ increases with decreasing E_r .
- As cavity-induced rate enhancement is often associated with the cavity mode frequency being "in resonance" with a certain energy scale of the cavity-free system, it is also of interest to consider the sensitivity of the rate enhancement to deviations of ω_p from ω_{max} . The FWHM of $F[\beta\hbar\omega_p;\ \beta\Delta E,\ \beta E_r]$ as a function of $\beta\hbar\omega_p$, for given $\beta\Delta E$ and βE_r can shed light on the resonance nature of the rate enhancement effect, in the sense that a

smaller fwhm would correspond to enhanced resonance-like behavior [see also Figure 4(b)]. In the case where βE_r is small and $-\beta \Delta E$ is large, the width of $F[\beta\hbar\omega_{\rm p};\,\beta\Delta E,\,\beta E_r]$ is dominated by the width of $k_{\rm A-D}^{\rm m}(\omega_{\rm p})$, which is determined by E_r (see Figure 1). In the complementary case where βE_r is large and $-\beta\Delta E$ is small, the width of $F[\beta\hbar\omega_{\rm p};\,\beta\Delta E,\,\beta E_r]$ is determined by how well the maxima of $\frac{k_{\rm A-D}^{\rm m}(\omega_{\rm p})}{k_{\rm A-D}^{\rm m}(0)}$ overlaps with the minima of $G(\beta\hbar\omega_{\rm p})$. More specifically, the smaller the $-\beta\Delta E$, the closer the two extrema and the narrower the $F[\beta\hbar\omega_{\rm p};\,\beta\Delta E,\,\beta E_r]$.

4. CONCLUSIONS

Rate theories based on equilibrium FGR have proven to be extremely useful for calculating the rates of a wide range of electronic energy and charge transfer processes that take place in molecular systems. In this paper, we introduced a general-purpose framework for estimating cavity-enabled modifications of such equilibrium FGR rate constants which requires the same inputs needed for estimating the corresponding cavity-free equilibrium FGR rate constants. Using this framework therefore makes it possible to bypass the need for an explicit simulation of the molecular system inside the cavity in order to estimate the effect of coupling to the cavity on the equilibrium FGR rate constant.

The proposed framework is based on the fact that the photonic DOF can be added to the Hamiltonian as nuclear-like DOF. Further assuming that the photonic and nuclear DOF are coupled to the electronic DOF, but not to each other, and taking advantage of the resulting separability of the nuclear/photonic terms in the Hamiltonian into purely nuclear and purely photonic terms is what makes it possible to calculate cavity-modified equilibrium FGR rate constants from cavity-free inputs.

Unlike other cavity-enabled effects, relatively weak coupling between molecular and cavity DOF can give rise to significant cavity-enabled modifications to the equilibrium FGR rate constant. This is because equilibrium FGR is based on treating the coupling between electronic states as a small perturbation (within the framework of second-order perturbation theory). Coupling between the electronic DOF and cavity modes can modify the coupling between electronic states when the molecular system is placed inside a cavity. Treating this additional electronic coupling as a small perturbation can therefore still give rise to significant modifications of the corresponding equilibrium FGR rate constant.

Marcus rate theory represents a highly successful example of an equilibrium-FGR-based rate theory with an extremely wide range of applicability. For this reason, we performed a detailed analysis of the proposed framework in the case where the cavity-free process can be described by Marcus rate theory. This analysis gave rise to closed form expressions that can be used for estimating cavity-enabled rate modifications and point to ways in which they can be optimized for the wide range of systems and processes to which Marcus theory is applicable.

While being rather general, the proposed framework is still based on a number of assumptions, including restricting ourselves to two electronic states, assuming that the molecular system is coupled to a single cavity mode and has no permanent dipole moment and neglecting nonequilibrium

effects. Work on extending the framework beyond those restrictive assumptions, while still maintaining its ability to produce cavity-modified rates from cavity-free inputs, is currently underway and will be reported in forthcoming publications.

AUTHOR INFORMATION

Corresponding Author

Eitan Geva — Department of Chemistry, University of Michigan, Ann Arbor, Michigan 48109, United States; orcid.org/0000-0002-7935-4586; Email: eitan@umich.edu

Authors

Maximilian A. C. Saller – Department of Chemistry, University of Michigan, Ann Arbor, Michigan 48109, United States

Yifan Lai — Department of Chemistry, University of Michigan, Ann Arbor, Michigan 48109, United States; Department of Chemistry, University of Rochester, Rochester, New York 14627, United States

Complete contact information is available at: https://pubs.acs.org/10.1021/acs.jpcc.2c08996

Author Contributions

§M.A.C.S. and Y.L. contributed equally to this work.

Notes

The authors declare no competing financial interest.

ACKNOWLEDGMENTS

E.G. acknowledges support from the NSF via Grants CHE-1800325 and CHE-2154114 and computational resources and services provided by the Advanced Research Computing at the University of Michigan, Ann Arbor.

REFERENCES

- (1) Tannor, D. J.; Rice, S. A. Coherent Pulse Sequence Control of Product Formation in Chemical Reactions. *Adv. Chem. Phys.* **2007**, *70*, 441–523.
- (2) Kosloff, R.; Rice, S. A.; Gaspard, P.; Tersigni, S.; Tannor, D. J. Wave Packet Dancing: Achieving Chemical Selectivity By Shaping Light Pulses. *Chem. Phys.* **1989**, *139*, 201–220.
- (3) Gordon, R. J.; Rice, S. A. Active Control of The Dynamics of Atoms and Molecules. *Annu. Rev. Phys. Chem.* **1997**, *48*, 601–641.
- (4) Assion, A.; Baumert, T.; Bergt, M.; Brixner, T.; Kiefer, B.; Seyfried, V.; Strehle, M.; Gerber, G. Control of Chemical Reactions by Feedback-Optimized Phase-Shaped Femtosecond Laser Pulses. *Science* 1998, 282, 919–922.
- (5) Rabitz, H.; Zhu, W. Optimal Control of Molecular Motion: Design Implementation and Inversion. *Acc. Chem. Res.* **2000**, *33*, 572–578.
- (6) Rice, S. A.; Zhao, M. Optical Control of Molecular Dynamics; Wiley: New York, 2000.
- (7) Levis, R. J.; Menkir, G. M.; Rabitz, H. Selective Bond Dissociation and Rearrangement With Optimally Tailored Strong Field Laser Pulses. *Science* **2001**, 292, 709–713.
- (8) Pearson, B. J.; White, J. L.; Weinacht, T. C.; Bucksbaum, P. H. Coherent Control Using Adaptive Learning Algorithms. *Phys. Rev. A* **2001**, *63*, 063412.
- (9) Rice, S. A.; Shah, S. P. Active Control of Product Selection in A Chemical Reaction: A View of The Current Scene. *Phys. Chem. Chem. Phys.* **2002**, *4*, 1683–1700.
- (10) Shapiro, M.; Brumer, P. Principles of The Quantum Control of Molecular Processes; Wiley: Hoboken, NJ, 2002.

- (11) McRobbie, P.; Geva, E. Coherent Control of Population Transfer via Linear Chirp in Liquid Solution: The Role of Motional Narrowing. *J. Phys. Chem. A* **2016**, *120*, 3015–3022.
- (12) Andrew, P.; Barnes, W. L. Förster energy transfer in an optical microcavity. *Science* **2000**, 290, 785–788.
- (13) Schwartz, T.; Hutchison, J.; Genet, C.; Ebbesen, T. Reversible Switching of Ultrastrong Light-Molecule Coupling. *Phys. Rev. Lett.* **2011**, *106*, 196405–4.
- (14) Hutchison, J.; Schwartz, T.; Genet, C.; Devaux, E.; Ebbesen, T. Modifying Chemical Landscapes by Coupling to Vacuum Fields. *Angew. Chem., Int. Ed.* **2012**, *51*, 1592–1596.
- (15) Hutchison, J.; Liscio, A.; Schwartz, T.; Canaguier-Durand, A.; Genet, C.; Palermo, V.; Samorì, P.; Ebbesen, T. Tuning the Work-Function Via Strong Coupling. *Adv. Mater.* **2013**, *25*, 2481–2485.
- (16) Törmä, P.; Barnes, W. Strong coupling between surface plasmon polaritons and emitters: A review. *Rep. Prog. Phys.* **2015**, 78, 013901–35.
- (17) Flick, J.; Ruggenthaler, M.; Appel, H.; Rubio, A. Kohn—Sham approach to quantum electrodynamical density-functional theory: Exact time-dependent effective potentials in real space. *Proc. Natl. Acad. Sci. U.S.A.* **2015**, *112*, 15285—15290.
- (18) Feist, J.; Garcia-Vidal, F. Extraordinary Exciton Conductance Induced by Strong Coupling. *Phys. Rev. Lett.* **2015**, *114*, 196402–5.
- (19) Schachenmayer, J.; Genes, C.; Tignone, E.; Pupillo, G. Cavity-Enhanced Transport of Excitons. *Phys. Rev. Lett.* **2015**, *114*, 196403–6.
- (20) Shalabney, A.; George, J.; Hutchison, J.; Pupillo, G.; Genet, C.; Ebbesen, T. Coherent coupling of molecular resonators with a microcavity mode. *Nat. Commun.* **2015**, *6*, 217.
- (21) Orgiu, E.; George, J.; Hutchison, J.; Devaux, E.; Dayen, J.; Doudin, B.; Stellacci, F.; Genet, C.; Schachenmayer, J.; Genes, C.; et al. Conductivity in organic semiconductors hybridized with the vacuum field. *Nat. Mater.* **2015**, *14*, 1123–1129.
- (22) Long, J.; Simpkins, B. Coherent Coupling between a Molecular Vibration and Fabry—Perot Optical Cavity to Give Hybridized States in the Strong Coupling Limit. ACS Photonics 2015, 2, 130–136.
- (23) Ebbesen, T. Hybrid Light-Matter States in a Molecular and Material Science Perspective. Acc. Chem. Res. 2016, 49, 2403–2412.
- (24) Thomas, A.; George, J.; Shalabney, A.; Dryzhakov, M.; Varma, S.; Moran, J.; Chervy, T.; Zhong, X.; Devaux, E.; Genet, C.; et al. Ground-State Chemical Reactivity under Vibrational Coupling to the Vacuum Electromagnetic Field. *Angew. Chem., Int. Ed.* **2016**, *128*, 11634–11638.
- (25) Zhong, X.; Chervy, T.; Wang, S.; George, J.; Thomas, A.; Hutchison, J.; Devaux, E.; Genet, C.; Ebbesen, T. Non-Radiative Energy Transfer Mediated by Hybrid Light-Matter States. *Angew. Chem., Int. Ed.* **2016**, *128*, 6310–6314.
- (26) Herrera, F.; Spano, F. Cavity-Controlled Chemistry in Molecular Ensembles. *Phys. Rev. Lett.* **2016**, *116*, 238301–6.
- (27) Casey, S.; Sparks, J. Vibrational Strong Coupling of Organometallic Complexes. J. Phys. Chem. C 2016, 120, 28138–28143.
- (28) Sanvitto, D.; Kéna-Cohen, S. The road towards polaritonic devices. *Nat. Mater.* **2016**, *15*, 1061–1073.
- (29) Kowalewski, M.; Bennett, K.; Mukamel, S. Cavity Femtochemistry: Manipulating Nonadiabatic Dynamics at Avoided Crossings. *J. Phys. Chem. Lett.* **2016**, *7*, 2050–2054.
- (30) Kowalewski, M.; Bennett, K.; Mukamel, S. Non-adiabatic dynamics of molecules in optical cavities. *J. Chem. Phys.* **2016**, *144*, 054309–9.
- (31) Flick, J.; Ruggenthaler, M.; Appel, H.; Rubio, A. Atoms and molecules in cavities, from weak to strong coupling in quantum-electrodynamics (QED) chemistry. *Proc. Natl. Acad. Sci. U.S.A.* **2017**, 114, 3026–3034.
- (32) Zhong, X.; Chervy, T.; Zhang, L.; Thomas, A.; George, J.; Genet, C.; Hutchison, J.; Ebbesen, T. Energy Transfer between Spatially Separated Entangled Molecules. *Angew. Chem., Int. Ed.* **2017**, *56*, 9034–9038.

- (33) Martínez-Martínez, L.; Ribeiro, R.; Campos-González-Angulo, J.; Yuen-Zhou, J. Can Ultrastrong Coupling Change Ground-State Chemical Reactions? *ACS Photonics* **2018**, *5*, 167–176.
- (34) Fregoni, J.; Granucci, G.; Coccia, E.; Persico, M.; Corni, S. Manipulating azobenzene photoisomerization through strong lightmolecule coupling. *Nat. Commun.* **2018**, *9*, 2613.
- (35) Sáez-Blázquez, R.; Feist, J.; Fernández-Domínguez, A.; García-Vidal, F. Organic polaritons enable local vibrations to drive long-range energy transfer. *Phys. Rev. B* **2018**, *97*, 241407–5.
- (36) Flick, J.; Welakuh, D.; Ruggenthaler, M.; Appel, H.; Rubio, A. Light–Matter Response in Nonrelativistic Quantum Electrodynamics. *ACS Photonics* **2019**, *6*, 2757–2778.
- (37) Galego, J.; Climent, C.; Garcia-Vidal, F.; Feist, J. Cavity Casimir-Polder Forces and Their Effects in Ground-State Chemical Reactivity. *Phys. Rev. X* **2019**, *9*, 021057–22.
- (38) Lather, J.; Bhatt, P.; Thomas, A.; Ebbesen, T.; George, J. Cavity Catalysis by Cooperative Vibrational Strong Coupling of Reactant and Solvent Molecules. *Angew. Chem., Int. Ed.* **2019**, *58*, 10635–10638.
- (39) Schäfer, C.; Ruggenthaler, M.; Appel, H.; Rubio, A. Modification of excitation and charge transfer in cavity quantum-electrodynamical chemistry. *Proc. Natl. Acad. Sci. U.S.A.* **2019**, *116*, 4883–4892.
- (40) Hoffmann, N.; Schäfer, C.; Rubio, A.; Kelly, A.; Appel, H. Capturing vacuum fluctuations and photon correlations in cavity quantum electrodynamics with multitrajectory Ehrenfest dynamics. *Phys. Rev. A* **2019**, *99*, 063819–9.
- (41) Hoffmann, N.; Schäfer, C.; Säkkinen, N.; Rubio, A.; Appel, H.; Kelly, A. Benchmarking semiclassical and perturbative methods for real-time simulations of cavity-bound emission and interference. *J. Chem. Phys.* **2019**, *151*, 244113–14.
- (42) Lacombe, L.; Hoffmann, N.; Maitra, N. Exact Potential Energy Surface for Molecules in Cavities. *Phys. Rev. Lett.* **2019**, *123*, 083201–6.
- (43) Mandal, A.; Huo, P. Investigating New Reactivities Enabled by Polariton Photochemistry. *J. Phys. Chem. Lett.* **2019**, *10*, 5519–5529.
- (44) Semenov, A.; Nitzan, A. Electron transfer in confined electromagnetic fields. *J. Chem. Phys.* **2019**, *150*, 174122.
- (45) Hoffmann, N.; Lacombe, L.; Rubio, A.; Maitra, N. Effect of many modes on self-polarization and photochemical suppression in cavities. *J. Chem. Phys.* **2020**, *153*, 104103–10.
- (46) Flick, J.; Rivera, N.; Narang, P. Strong light-matter coupling in quantum chemistry and quantum photonics. *Nanophotonics* **2018**, *7*, 1479–1501.
- (47) Gu, B.; Mukamel, S. Manipulating nonadiabatic conical intersection dynamics by optical cavities. *Chem. Sci.* **2020**, *11*, 1290–1298.
- (48) Mandal, A.; Krauss, T.; Huo, P. Polariton-Mediated Electron Transfer via Cavity Quantum Electrodynamics. *J. Phys. Chem. B* **2020**, 124, 6321–6340.
- (49) Chowdhury, S.; Mandal, A.; Huo, P. Ring polymer quantization of the photon field in polariton chemistry. *J. Chem. Phys.* **2021**, *154*, 044109–11.
- (50) Saller, M.; Kelly, A.; Geva, E. Benchmarking Quasiclassical Mapping Hamiltonian Methods for Simulating Cavity-Modified Molecular Dynamics. *J. Phys. Chem. Lett.* **2021**, *12*, 3163–3170.
- (51) Saller, M. A. C.; Lai, Y.; Geva, E. An Accurate Linearized Semiclassical Approach for Calculating Cavity-Modified Charge Transfer Rate Constants. *J. Phys. Chem. Lett.* **2022**, *13*, 2330–2337.
- (52) Basov, D.; Asenjo-Garcia, A.; Schuck, P.; Zhu, X.; Rubio, A. Polariton panorama. *Nanophotonics* **2020**, *10*, 549–577.
- (53) Dicke, R. Coherence in spontaneous radiation processes. *Phys. Rev.* **1954**, *93*, 99–110.
- (54) Jaynes, E.; Cummings, F. Comparison of quantum and semiclassical radiation theories with application to the beam maser. *Proc. IEEE* **1963**, *51*, 89–109.
- (55) Tavis, M.; Cummings, F. Approximate solutions for an N-molecule-radiation-field Hamiltonian. *Phys. Rev.* **1969**, *188*, 692–695.
- (56) Houdre, R.; Stanley, R.; Ilegems, M. Vacuum-field Rabi splitting in the presence of inhomogeneous broadening: Resolution of

- a homogeneous linewidth in an inhomogeneously broadened system. *Phys. Rev. A* **1996**, *53*, 2711–2715.
- (57) Walther, H.; Varcoe, B.; Englert, B.-G.; Becker, T. Cavity quantum electrodynamics. *Rep. Prog. Phys.* **2006**, *69*, 1325–1382.
- (58) Garraway, B. The Dicke model in quantum optics: Dicke model revisited. P. R. Soc. A: Math. Phys. 2011, 369, 1137–1155.
- (59) Li, T.; Subotnik, J.; Nitzan, A. Cavity molecular dynamics simulations of liquid water under vibrational ultrastrong coupling. *Proc. Natl. Acad. Sci. U.S.A.* **2020**, *117*, 18324–18331.
- (60) Haugland, T.; Schäfer, C.; Ronca, E.; Rubio, A.; Koch, H. Intermolecular interactions in optical cavities: An ab initio QED study. *J. Chem. Phys.* **2021**, *154*, 094113.
- (61) Li, T.; Nitzan, A.; Subotnik, J. Cavity molecular dynamics simulations of vibrational polariton-enhanced molecular nonlinear absorption. *J. Chem. Phys.* **2021**, *154*, 094124.
- (62) Li, T.; Nitzan, A.; Subotnik, J. Collective Vibrational Strong Coupling Effects on Molecular Vibrational Relaxation and Energy Transfer: Numerical Insights via Cavity Molecular Dynamics Simulations. *Angew. Chem., Int. Ed.* **2021**, *60*, 15533–15540.
- (63) Fischer, E.; Anders, J.; Saalfrank, P. Cavity-altered thermal isomerization rates and dynamical resonant localization in vibropolaritonic chemistry. *J. Chem. Phys.* **2022**, *156*, 154305.
- (64) Wang, D.; Neuman, T.; Yelin, S.; Flick, J. Cavity-Modified Unimolecular Dissociation Reactions via Intramolecular Vibrational Energy Redistribution. *J. Phys. Chem. Lett.* **2022**, *13*, 3317–3324.
- (65) Li, T.; Nitzan, A.; Subotnik, J. Polariton relaxation under vibrational strong coupling: Comparing cavity molecular dynamics simulations against Fermi's golden rule rate. *J. Chem. Phys.* **2022**, *156*, 134106
- (66) Mandal, A.; Li, X.; Huo, P. Theory of vibrational polariton chemistry in the collective coupling regime. *J. Chem. Phys.* **2022**, *156*, 014101.
- (67) Li, T.; Chen, H.-T.; Nitzan, A.; Subotnik, J. Quasiclassical modeling of cavity quantum electrodynamics. *Phys. Rev. A* **2020**, *101*, 033831–17.
- (68) Shi, Q.; Geva, E. Nonradiative electronic relaxation rate constants from approximations based on linearizing the path-integral forward-backward action. *J. Phys. Chem. A* **2004**, *108*, 6109–6116.
- (69) Nitzan, A. Chemical Dynamics in Condensed Phases; Oxford University Press: New York, 2006.
- (70) Sun, X.; Geva, E. Equilibrium Fermi's Golden Rule Charge Transfer Rate Constants in the Condensed Phase: The Linearized Semiclassical Method vs Classical Marcus Theory. *J. Phys. Chem. A* **2016**, *120*, 2976–2990.

☐ Recommended by ACS

A Mean-Field Treatment of Vacuum Fluctuations in Strong Light–Matter Coupling

Ming-Hsiu Hsieh, Roel Tempelaar, et al.

JANUARY 31, 2023

THE JOURNAL OF PHYSICAL CHEMISTRY LETTERS

RFAD 🗹

Optimal Mode Combination in the Multiconfiguration Time-Dependent Hartree Method through Multivariate Statistics: Factor Analysis and Hierarchical Clustering

David Mendive-Tapia, Oriol Vendrell, et al.

JANUARY 30, 2023

JOURNAL OF CHEMICAL THEORY AND COMPUTATION

READ 🗹

Carbonate Reservoir Quality Variations in Basins with a Variable Sediment Influx: A Case Study from the Balkassar Oil Field, Potwar, Pakistan

Muhammad Raiees Amjad, Ahmed Elbeltagi, et al.

JANUARY 18, 2023

ACS OMEGA

READ **C**

Broadband Enhancement of Optical Nonlinearity in a Plasmonic Nanocavity Coupled with an Epsilon-Near-Zero Film

Feilian Zhang, Yihang Chen, et al.

FEBRUARY 08, 2023

THE JOURNAL OF PHYSICAL CHEMISTRY C

READ 🗹

Get More Suggestions >